Bispecific antibody CD73xEpCAM selectively inhibits the adenosine-mediated immunosuppressive activity of carcinoma-derived extracellular vesicles

Ploeg, Emily M; Ke, Xiurong; Britsch, Isabel; Hendriks, Mark A J M; Van der Zant, Femke A; Kruijff, Schelto; Samplonius, Douwe F; Zhang, Hao; Helfrich, Wijnand

Published in:
Cancer letters

DOI:
10.1016/j.canlet.2021.08.037

Publication date:
2021

Cancer Letters 521 (2021) 109–118

Contents lists available at ScienceDirect

Cancer Letters

journal homepage: www.elsevier.com/locate/canlet

Bispecific antibody CD73xEpCAM selectively inhibits the adenosine-mediated immunosuppressive activity of carcinoma-derived extracellular vesicles

Emily M. Ploeg [a,1], Xiurong Ke [a,b,1], Isabel Britsch [a], Mark A.J.M. Hendriks [a], Femke A. Van der Zant [a], Schelto Kruijff [a], Douwe F. Samplonius [a], Hao Zhang [c,**], Wijnand Helfrich [a,*]

[a] University of Groningen, University Medical Center Groningen (UMCG), Department of Surgery, Laboratory for Translational Surgical Oncology, Groningen, the Netherlands
[b] Shantou University Medical College, Shantou, Guangdong, China
[c] Institute of Precision Cancer and Pathology, Department of Pathology, School of Medicine, Department of General Surgery, First Affiliated Hospital, Jinan University, Guangzhou, Guangdong, China

ARTICLE INFO

Keywords:
Bifunctional antibody
Tumor exosomes
Ecto-5′-nucleotidase
Immune checkpoint
Cancer immunotherapy

ABSTRACT

Tumor-derived extracellular vesicles (EVs) carry potent immunosuppressive factors that affect the antitumor activities of immune cells. A significant part of the immunoinhibitory activity of EVs is attributable to CD73, a GPI-anchored ecto-5′-nucleotidase involved in the conversion of tumor-derived proinflammatory extracellular ATP (eATP) to immunosuppressive adenosine (ADO). The CD73-antagonist antibody oleclumab inhibits cell surface-exposed CD73 and is currently undergoing clinical testing for cancer immunotherapy. However, a strategy to selectively inhibit CD73 exposed on EVs is not available. Here, we present a novel bispecific antibody (bsAb) CD73xEpCAM designed to bind with high affinity the common EV surface marker EpCAM and concurrently inhibit CD73. Unlike oleclumab, bsAb CD73xEpCAM potently inhibited the immunosuppressive activity of EVs from $CD73^{pos}$/$EpCAM^{pos}$ carcinoma cell lines and patient-derived colorectal cancer cells. Taken together, selective blockade of EV-exposed CD73 by bsAb CD73xEpCAM may be useful as an alternate or complementary targeted approach in cancer immunotherapy.

1. Introduction

Exosomes are endosome-derived nanoscale (30–150 nm) extracellular vesicles (EVs) that are actively secreted by numerous cell types, including malignant tumor cells. High levels of tumor-derived EVs can be detected in bodily fluids of cancer patients [1](2). Typically, tumor-derived EVs carry a unique repertoire of cancer-associated (cell surface) proteins, lipids, RNA (miRNAs, mRNAs, lncRNAs) and DNA that reflects the cancer cells of origin. This repertoire may include molecules that are able to mediate pro-tumoral effects including angiogenesis, proliferation, metastasis [3]. Importantly, emerging evidence indicates that EVs also expose immunoinhibitory molecules like PD-L1 which protect cancer cells from elimination by immune surveillance [4]. Recently, it was shown that a significant part of the immunoinhibitory activity of EVs is attributable to ectonucleotidase CD73 [5–7].

Normally, ectonucleotidases CD39 and CD73 are involved in down-

Abbreviations: EVs, extracellular vesicles; eATP, extracellular adenosine triphosphate; ADO, adenosine; AMP, adenosine monophosphate; TME, tumor microenvironment; EpCAM, epithelial cell adhesion molecule; bsAb, bispecific antibody; sCD73, soluble CD73; sEpCAM, soluble EpCAM; Pi, inorganic phosphate; HIPEC, hyperthermia intraperitoneal chemotherapy; PBMC, peripheral blood mononuclear cell.

* Corresponding author. Department of Surgery, Laboratory for Translational Surgical Oncology, University Medical Center Groningen, Hanzeplein 1, 9713 GZ, Groningen, the Netherlands.
** Corresponding author. Institute of Precision Cancer and Pathology, School of Medicine, Jinan University, 601 Huangpu Avenue West, Guangzhou, Guangdong 510632, China.
E-mail addresses: haolabcancercenter@163.com (H. Zhang), w.helfrich@umcg.nl (W. Helfrich).
[1] Emily M. Ploeg, Xiurong Ke contributed equally to this work.

https://doi.org/10.1016/j.canlet.2021.08.037
Received 9 June 2021; Received in revised form 24 August 2021; Accepted 26 August 2021
Available online 28 August 2021

regulation of pro-inflammatory immune responses by sequentially dephosphorylating extracellular ATP (eATP) into adenosine (ADO), which is one of the most powerful immunosuppressive molecules in the human body. In this process, CD73 is rate limiting in the conversion of adenosine monophosphate (AMP) to ADO. This catalysis step results in a rapid local increase of ADO levels, both in and outside of the tumor microenvironment (TME). Subsequently, elevated ADO levels engage the immunosuppressive actions of adenosine A2A and A2B receptors on locally present immune cells, thereby providing a self-limiting and counterbalancing mechanism to timely and locally resolve the immune response [8].

Due to high metabolic stress, cancer cells typically excrete high levels of pro-inflammatory eATP. However, this eATP is rapidly hydrolyzed to anti-inflammatory ADO by cancer cell surface-overexpressed CD73. These ADO molecules may diffuse from the TME, thereby forming an extratumoral immunosuppressive 'halo' that is able to chronically suppress the anticancer immune activities of a broad variety of immune effector cells [9,10]. Therapeutic blockade of the CD73/ADO immune checkpoint on cancer cells using antagonistic antibody oleclumab appears to be a promising approach to overcome immunosuppression by restoring ADO-suppressed anticancer activities of various immune effector cells [11].

Besides cell-bound CD73, cancer cells secrete EVs that may expose high levels of CD73 in the TME [5–7]. Nanoscale vesicles like EVs can easily propagate to tumor-draining lymph nodes and locally inhibit anticancer immune responses [12,13]. Moreover, EVs can reach the systemic circulation and subsequently contribute to a cancer-favorable microenvironment in the pre-metastatic niches. Additionally, EVs may fuse with the plasma membrane of (cancer) cells, providing these cells with CD73-based immunoinhibitory and pro-oncogenic activities [14]. Consequently, CD73-exposing EVs may prime an initially immunocompetent organ microenvironment and render it amenable for subsequent metastatic cell colonization and/or tumor progression. Therefore, blockade of CD73 on EVs may be useful as an approach to overcome ADO-mediated immune suppression in various malignancies. In this respect, it is noteworthy that the capacity of oleclumab to inhibit CD73 activity exposed on EVs has not been evaluated in any detail. Moreover, thus far therapeutic approaches to selectively inhibit CD73 exposed on EVs have not been developed. In this respect, bispecific antibodies (bsAbs) appear better suited to improve efficacy and safety of cancer immunotherapy as they can be engineered to more selectively direct immune checkpoint blockade to cancer cells and derived EVs [15–18].

For the current study, we developed bsAb CD73xEpCAM with engineered tetravalent bispecific capacity to concurrently bind to CD73 and Epithelial Cell Adhesion Molecule (EpCAM), in order to promote selective blockade of CD73 exposed on $CD73^{pos}$/$EpCAM^{pos}$ carcinoma cells and carcinoma-derived EVs. We selected the clinically relevant pan-carcinoma target antigen EpCAM as the tumor-directing second specificity of our CD73-blocking bsAb CD73xEpCAM. EpCAM is selectively overexpressed on broad variety of human carcinomas [19], and abundantly exposed on carcinoma-derived EVs [20,21]. Importantly, EpCAM expression in nonmalignant tissue is low and mostly limited to the basolateral surface of epithelia, which would further reduce on-target/off tumor binding upon intravenously administration of bsAb CD73xEpCAM.

Here we demonstrate that due to the concurrent binding of bsAb CD73xEpCAM to CD73 and EpCAM, it binds with higher affinity to EpCAM-expressing cells and EVs. Moreover, unlike oleclumab, bsAb CD73xEpCAM has potent capacity to selectively inhibit the enzyme activity of EVs derived from EpCAM-expressing cancer cells. Importantly, bsAb CD73xEpCAM potently inhibited CD73 exposed on EVs isolated from a $CD73^{pos}$/$EpCAM^{pos}$ colon carcinoma patient with advanced disease.

Additionally, bsAb CD73xEpCAM showed remarkable capacity to restore the anticancer activity of EV-suppressed T cells. This unique mode-of-action is not available in oleclumab or any other CD73-blocking antibody. To the best of our knowledge, this is the first report on a bsAb-based approach that selectively and potently inhibits immune suppression mediated by both cancer cell- and EVs-exposed CD73. BsAb CD73xEpCAM may be useful as an alternative or complementary approach for cancer immunotherapy to overcome CD73-induced immunosuppression.

2. Materials and methods

2.1. Antibodies and reagents

Fluorescently labeled secondary antibody used for flowcytometry: goat anti-human IgG APC (SouthernBiotech).

Unconjugated primary antibodies used for immunoblot analysis: sheep-anti-human CD73 (R&D), rabbit-anti-human-EpCAM (Abcam), rabbit-anti-human PD-L1 (R&D), rabbit-anti-human-calnexin (Abcam), rabbit-anti-human-CD9 (Abcam), rabbit-anti-human-TSG101 (Abcam), rabbit-anti-human/mouse-β-Actin (Abcam).

Horseradish peroxidase-conjugated secondary antibodies used for immunoblot analysis: Rabbit-anti-sheep-IgG (Thermofisher), goat-anti-rabbit-IgG (Dako).

The following reagents were used: recombinant soluble human CD73 (sCD73) (Abcam), recombinant soluble human EpCAM (sEpCAM) (Abcam), CFSE CellTrace Far Red cell proliferation kit (Thermofisher), fluorescent caspase 3/8–488 probe (Biotium). IFNγ was measured using appropriate ELISA kit (eBioscience).

2.2. Cell lines and transfectants

Cell lines H292, OvCAR3, DLD1, PC-3M and CHO–K1 cells were obtained from the American Type Culture Collection (ATCC, Manassas, VA). Cells were cultured in RPMI-1640 or DMEM (Lonza) as indicated, supplemented with 10% fetal calf serum (FCS, Thermofisher) at 37 °C in a humidified 5% CO_2 atmosphere. CHO–K1 cells were cultured in GMEM (First Link), supplemented with 5% dialyzed FBS (Sigma Aldrich).

CHO.CD73 cells stably expressing human CD73 were generated by lipofection (Fugene-HD, Promega) using plasmids containing cDNAs encoding human CD73 (Origene). Likewise, CHO.EpCAM cells were generated by lipofection using plasmids containing cDNAs encoding human EpCAM (Sino Biological).

CRISPR-Cas9 CD73-knockout (KO) cells were generated by transfection of H292 cells with pSpCas9 BB-2A-GFP (PX458) plasmid (Addgene plasmid #48138) containing the CD73-targeting sgRNA 5′-GCAGCACGTTGGGTTCGGCG-3' [22]. Likewise, EpCAM-KO H292 cells were generated by transfection of H292 cells with pSpCas9 BB-2A-GFP (PX458) plasmid containing the EpCAM-targeting sgRNA 5′-TAATGTTATCACTATTGATC-3' [23].

2.3. Construction of bsAb CD73xEpCAM-IgG2silent

DNA fragments encoding scFvCD73 and scFvEpCAM were generated by commercial gene synthesis service (Genscript) based on published VH and VL sequence data. For construction and production of bsAb CD73xEpCAM-IgG2silent, we used eukaryotic expression plasmid pbsAb, which contains 3 consecutive multiple cloning sites (MCS). MCS#1 and MCS#2 are interspersed by a 22 amino acid flexible linker [24]. MCS#1, MCS#2 were used for directional and in-frame insertion of DNA fragments encoding scFvCD73, scFvEpCAM, and MCS#3 for insertion of DNA fragments encoding human Fc IgG2s [25] (Fig. 2A). Analogously, pbsAb-CD73xMock-IgG2s encoding bsAb CD73xMock-IgG2s was constructed by replacing scFvEpCAM in pbsAb-CD73xEpCAM-IgG2s by scFvMCSP directed against CSPG4 [15]. Likewise, pbsAb-MockxEpCAM-IgG2s encoding bsAb MockxEpCAM-IgG2s was constructed by replacing scFvCD73 in pbsAb-CD73xEpCAM-IgG2s by scFv4-4-20 directed against fluorescein [17].

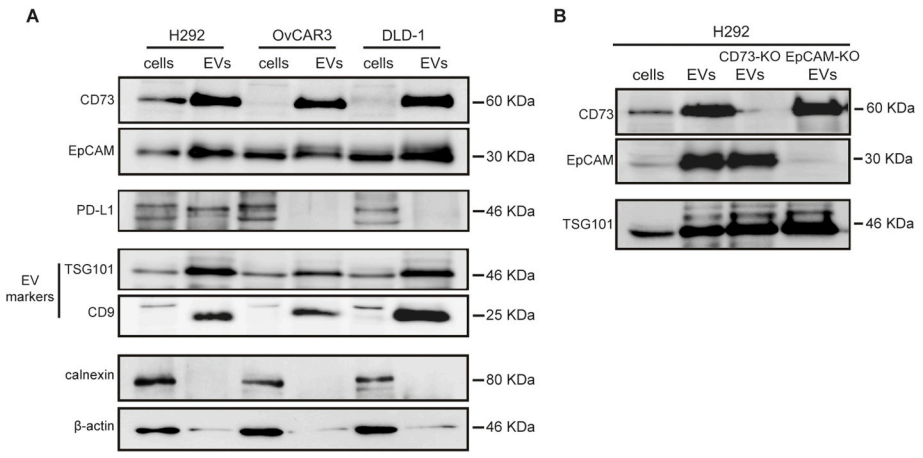

Fig. 1. CD73 and EpCAM are highly abundant on EVs. (A) Representative images of immunoblot analysis for presence of CD73, EpCAM, PD-L1, CD9, TSG101, calnexin and β-actin in cancer cells H292, OvCAR3, DLD1 and corresponding EVs. (B) CD73, EpCAM and TSG101 in EVs derived from parental H292, H292$^{CD73-KO}$ and H292$^{EpCAM-KO}$ cells, respectively. 20 μg protein of each sample (both cells and EVs) was loaded. Of note: The apparent difference in EpCAM signal in H292 cells between Fig. 1A and B is due to a reduction of exposure time during bioluminescent-based detection to prevent overexposure of the very high EpCAM signal from H292-derived EVs in Fig. 1B.

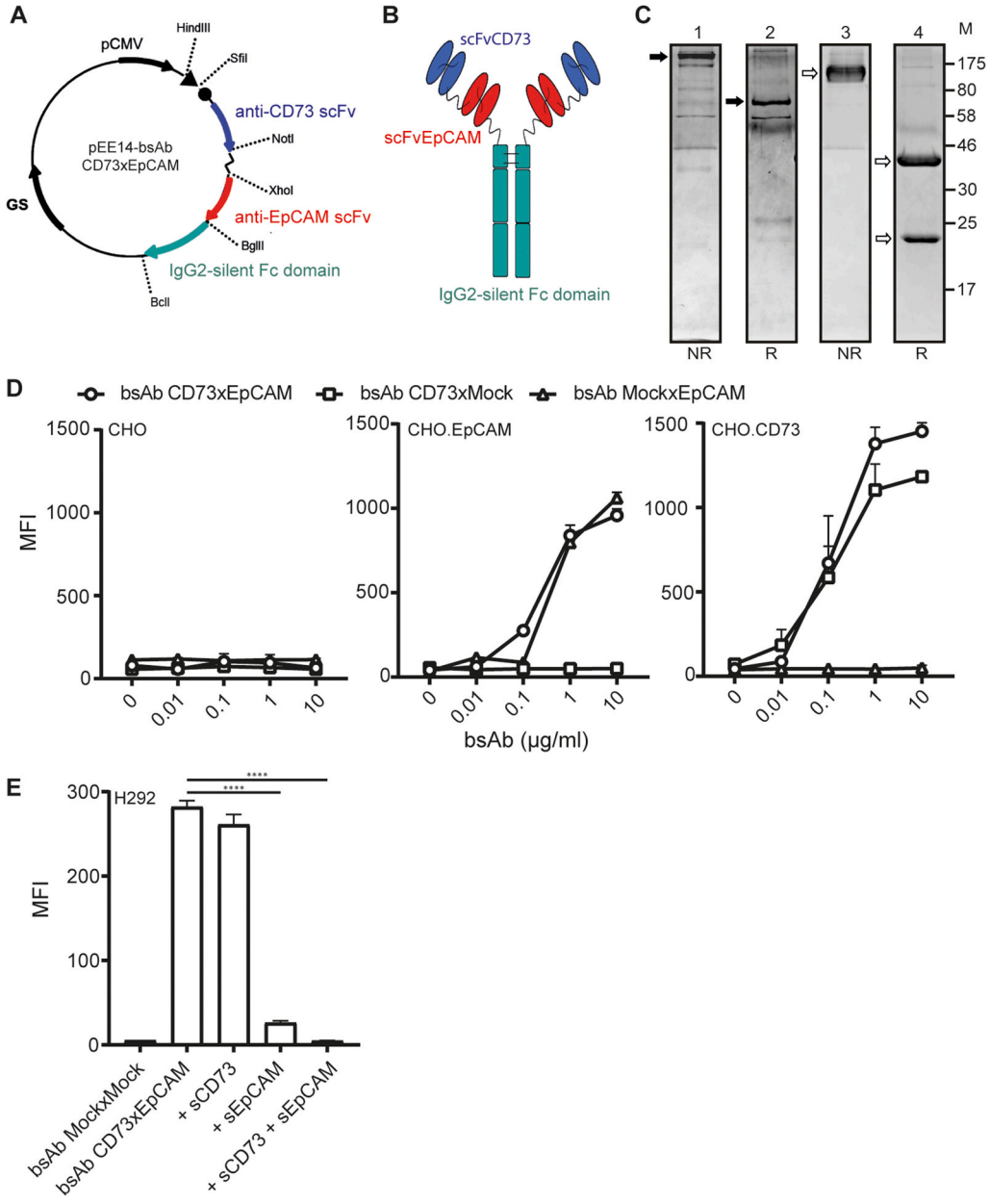

Fig. 2. BsAb CD73xEpCAM has dual binding specificity for CD73 and EpCAM. (A) Topology of expression plasmid pbsAb CD73xEpCAM-IgG2s. (B) Schematic depiction of bsAb CD73xEpCAM. (C) bsAb CD73xEpCAM (lane 1 and 2) or oleclumab (lane 3 and 4) (5 μg each) were separated by an SDS-PAGE gel using non-reducing (NR) and reducing (R) conditions. Under non-reducing conditions CD73xEpCAM migrated as a single protein band with an apparent molecular weight of 175 kDa (lane 1), which dropped to 75 kDa when separated under reducing conditions (lane 2). This is in good agreement with the calculated molecular weight of 83 kDa for CD73xEpCAM monomer and the proposed disulfide-stabilized dimeric single chain composition of the native protein. Oleclumab showed the expected heterodimeric composition of heavy and light chain characteristic for conventional antibodies (lane 3 and 4). The protein bands of bsAb CD73xEpCAM are indicated by solid black arrows and bands of oleclumab by open black arrows. (D) Comparison of dose-dependent binding of bsAb CD73xEpCAM, bsAb CD73xMock and bsAb MockxEpCAM to CHO, CHO.EpCAM and CHO.CD73 cells, respectively. (E) Competitive binding assay in which bsAb CD73xEpCAM was pretreated with excess amounts of soluble CD73 (sCD73), soluble EpCAM (sEpCAM) or a combination thereof (10 μg) prior to incubation with H292 cancer cells. Graphs D-E were analyzed by flow cytometry. All graphs represent mean ± SD. Statistical analysis in graphs E was performed using un-paired T test (****$p < .0001$). M = marker in graph C.

2.4. Production of recombinant bsAbs

The Expi293 expression system (ThermoFisher) was used to produce bsAbs CD73xEpCAM-IgG2s, CD73xMock-IgG2s and MockxEpCAM-IgG2s. Briefly, Expi293 cells were transfected with plasmid encoding the bsAb of choice and cultured on a shaker platform (125 rpm) at 37 °C, 8% CO_2 for 7 d. Next, conditioned culture supernatant was harvested and cleared by centrifugation (4000×*g* for 30 min), after which bsAbs were purified using an HiTrap Mabselect column connected to an ÄKTA Start chromatography system (GE Healthcare Life Sciences).

2.5. SDS-PAGE analysis of bsAb CD73xEpCAM

Purified bsAb CD73xEpCAM and oleclumab (5 μg) were separated by SDS-PAGE (10% acrylamide) under reducing or non-reducing conditions, followed by staining of the gel with Coomassie brilliant blue. The calculated molecular weight of bsAb CD73xEpCAM adds up to 166 kDa.

2.6. Tumor-derived EVs and HIPEC patient-derived EVs isolation

H292, OvCAR3 and DLD-1 cells were cultured as indicated above with 10% FCS until confluency of 80–90% was reached. Subsequently, cancer cells were cultured using serum free medium for 48 h after which EVs were isolated from the spent culture medium by stepwise (ultra) centrifugation.

Cancer patient-derived EVs were isolated from rinsing fluid obtained during Hyperthermia Intraperitoneal Chemotherapy (HIPEC) surgery after written informed consent (institutional approval by University Medical Center Groningen, nr. METc2012/330). After surgical tumor resection, the abdomen was rinsed with Mitomycin C for 90 min. Subsequently, the surgeon rinsed the abdomen with 1.5 L saline and 240 ml of rinsing fluid was collected directly from the patient's abdomen and promptly used for EVs isolation.

Briefly, spent culture medium or HIPEC rinsing fluid were centrifuged at 300×*g* at 4 °C for 15 min to remove dead cells and debris, followed by 3000×*g* centrifugation at 4 °C for 25 min to remove apoptotic bodies. The supernatant was filtrated using a 0.2 μm pore filter to remove large vesicles. Next, supernatant was subjected to ultracentrifugation at 110,000×*g* at 4 °C for 2 h in a SW 32 Ti Rotor Swinging Bucket rotor (k factor of 204, Beckman Coulter) to sediment EVs. EVs pellets were washed with PBS and recovered by another round of ultracentrifugation.

2.7. Nanoparticle Tracking Analysis of EVs

Size distribution and concentration were analyzed by the Nanosight LM14 apparatus, equipped with a blue laser (405 nm) and a high sensitivity digital CMOS camera. Briefly, EVs were diluted 500 times in particle-free PBS and injected into the LM14 unit with a 1-ml sterile syringe. EVs were visualized by laser light scattering and Brownian motion was captured in a video of 60 s. In total 5 videos were captured for each individual sample to provide a representative concentration measurement. Videos were analyzed using NTA software 3.0 to provide nanoparticle concentrations and size distribution profiles.

2.8. Immunoblot analysis

Lysed cell samples and isolated EVs were determined for protein content using the Bradford method after which samples with equal protein content (20 μg) were subjected to SDS/PAGE. In short, samples were mixed with 4x Laemmli sample buffer (containing 355 mM 2-mercaptoethanol) and heated at 95 °C for 5 min. Subsequently, the separated proteins were transferred to a 0.45 μm nitrocellulose membrane. Separate lanes of the membrane were incubated with indicated primary antibodies at 4 °C for 16 h and subsequently incubated with an appropriate horseradish peroxidase-conjugated secondary antibody at room temperature for 2 h. Immunoreactive bands were visualized with SuperSignal West Pico Chemiluminescent Substrate (Thermofisher).

2.9. Assessment dual binding activity of bsAb CD73xEpCAM to cells

Samples of CHO, CHO.CD73 or CHO.EpCAM cells (each 5×10^4 cells/ml in culture medium) were incubated with increasing concentrations (0.01–10 μg/ml) of bsAbs CD73xEpCAM, CD73xMock or MockxEpCAM at 4 °C for 45 min. Unbound bsAb was removed by washing the incubated cells three times with cold PBS, after which cells were re-incubated with an APC-labeled secondary anti-human-Ig-antibody at 4 °C for 45 min and then washed again. Binding data of the respective bsAbs were acquired using a Guava EasyCyte 6/2L flow cytometer (Merck Millipore) and analyzed by applying GuavaSoft 3.2 software.

In short, viable cells were gated in region 1 (R1) based on forward (X-axis)/sideward (Y-axis) scatter profile. Binding of bsAb CD73xEpCAM or controls to R1-gated cells is indicated by cell count on Y-axis and Mean Fluorescent Intensity (MFI) on the X-axis using the Red-R channel settings of the flow cytometer.

The overall binding strength (avidity) of bsAb CD73xEpCAM (1 μg/ml) towards $EpCAM^{pos}/CD73^{pos}$ H292 cells was accessed in the competing presence of recombinant sCD73, recombinant sEpCAM or a combination thereof (each 10 μg) at 4 °C for 20 min. Binding of bsAb CD73xEpCAM to H292 cells was evaluated by flowcytometry using an APC-labeled anti-human-Ig-antibody essentially as described above.

2.10. Serum, pH and temperature stability of bsAb CD73xEpCAM and oleclumab

Assessment of serum stability: In short, bsAb CD73xEpCAM and oleclumab (each 5 μg) were stored in 100% human AB serum (Corning) at 37 °C for 0, 2 and 7 d.

Assessment of pH stability: In short, bsAb CD73xEpCAM and oleclumab (each 5 μg) were stored in 20 mM acetate buffer, at pH 4, 5, 6 or 7 at 4 °C for 0, 2 and 7 d.

Assessment of thermostability: In short, bsAb CD73xEpCAM and oleclumab (each 5 μg) were stored in PBS at −20, 4 and 37 °C for 0, 2 and 7 d.

At the indicated timepoints remaining capacities to bind to CD73 and inhibit CD73 enzyme activity were evaluated using H292 cells essentially as described sections 2.9 and 2.11, respectively.

2.11. Assessment capacity of bsAb CD73xEpCAM to inhibit cancer cell-expressed CD73

The enzyme activity of CD73 was assessed using a colorimetric malachite green-based Pi assay kit (ab65622, Abcam), which detects the amount of inorganic phosphate (Pi) formed during the hydrolysis of AMP to adenosine (ADO). In short, H292 cells were treated with bsAb CD73xEpCAM or indicated controls (1 μg/ml) at 37 °C for 40 min. Subsequently, cells were washed (20 mM HEPES, 120 mM NaCl, 5 mM KCl, 2 mM MgCl2, 10 mM Glucose, pH 7.4) to remove phosphates and incubated with AMP (100 μM, Sigma-Aldrich) at 37 °C for 40 min. The supernatant was mixed with phosphate reagent and color development was evaluated by measuring the absorbance at 650 nm using a microplate reader (VERSA max, Molecular Devices) and corrected by subtracting background levels.

The % of enzyme inhibition was calculated by the following formula:

$$\%\ of\ CD73\ enzyme\ inhibition = 100 - \left(\left(\frac{X}{OD650max}\right) * 100\right)$$

X = the OD value measured in a given experiment minus the background (OD650exp- OD650background). OD650max = the amount of Pi present in the conditioned supernatant in the absence of bsAb.

2.12. Assessment capacity of bsAb CD73xEpCAM to inhibit EVs-exposed CD73

H292 derived-EVs (10 μg) or HIPEC patient-derived EVs (10 μg) were incubated with bsAb CD73xEpCAM or control antibodies (1 μg/ml) at 4 °C for 40 min. Subsequently, EVs were washed using a 100K MWCO Amicon Ultra 0.5 ml centrifugal filter to remove phosphates and then 0.5 μg EV were incubated with AMP (100 μM) at 37 °C for 40 min. Pi produced by CD73-mediated hydrolysis of AMP was assessed using colorimetric malachite green-based Pi assay. Where indicated, H292 derived-EVs were incubated with a dose range (0.25–1 μg/ml) of bsAb CD73xEpCAM in the presence (or absence) of sEpCAM (10 μg) at 4 °C for 40 min.

2.13. Assessment capacity of bsAb CD73xEpCAM to restore proliferation capacity of ADO-suppressed T cells

Peripheral Blood Mononuclear Cells (PBMCs) obtained from healthy donors were labeled with cell permeable fluorescent dye CFSE-FarRed (Thermofisher) according to manufacturer protocol and re-suspended in RPMI-1640. Next, CFSE-labeled PBMCs were cultured in medium supplemented with H292 parental or CD73-KO derived-EVs (50 μg EV/10^6 PBMCs) in the presence, or absence, of bsAb CD73xEpCAM or controls (1 μg/ml) at 37 °C for 3 d. Subsequently, PBMCs were treated (or not) with AMP (100 μM) at 37 °C for 40 min and activated by addition of T cell activation/expansion beads (Miltenybiotec) in a cell to bead ratio of 1:2. Live cell imaging technology (IncuCyte) was used to evaluate the number and size of T cell clusters by taking pictures every 6 h at 10 x magnification. The area (μm^2/image) of activated T cell clusters was quantified using IncuCyte software 2019B.

2.14. Assessment capacity of bsAb CD73xEpCAM to restore anticancer activity of ADO-suppressed T cells

Freshly isolated PBMCs were cultured in medium supplemented (or not) with H292 parental or CD73-KO derived-EVs (50 μg EV/10^6 PBMCs) in the presence, or absence, of bsAb CD73xEpCAM or controls (1 μg/ml) at 37 °C for 3 d. Next, PBMCs were incubated (or not) with AMP (100 μM) at 37 °C for 24 h. Subsequently, the T cells present in the PBMC population were stimulated and re-directed to kill EpCAM-expressing PC-3M prostate cancer cells using an EpCAM-directed/CD3-agonistic bispecific antibody (BIS-1) in an effector (E) to target (T) cell ratio of 4:1 [26]. Subsequently, effector and target cells were co-cultured for 2 d in the presence of a conditionally fluorescent caspase 3/8–488 probe (Biotium). Live cell imaging technology (IncuCyte) was used to evaluate induction of apoptotic cancer cell death by taking pictures every 1.5 h at 10x magnification. Apoptotic cancer cell death was calculated as caspase-488 count per image using IncuCyte software 2019B.

2.15. Statistical analysis

Statistical analysis was done by (multiple) T-test or one-way ANOVA followed by Tukey post-hoc test, as indicated using Prism software. $P < .05$ was defined as a statistically significant difference. Where indicated ns = $P > .05$; * = $P < .05$; ** = $P < .01$; *** = $P < .001$; **** = $P < .0001$.

3. Results

3.1. CD73 and EpCAM are abundantly present on EVs

EVs derived from cancer cell lines H292 (non-small cell lung cancer), OvCAR3 (ovarian cancer) and DLD1 (colon carcinoma) were purified by stepwise (ultra)centrifugation. Nanoparticle Tracking Analysis (NTA) indicated that the size of these EVs ranged between 118 nm and 136 nm (Supplementary Fig. 1). Immunoblot analysis indicated that EV markers CD9 and TSG101 were present in EVs, whereas endoplasmic reticulum protein calnexin was only present in cellular extracts, demonstrating that the isolated vesicles are indeed EVs and not contaminated with cellular protein (Fig. 1A). Compared to the originating cancer cell extracts, EpCAM and immune checkpoint CD73, but not PD-L1, were selectively enriched in EVs (Fig. 1A). As expected, CRISPR/Cas9-mediated CD73-KO and EpCAM-KO H292 cells produced EVs devoid of CD73 and EpCAM exposure, respectively (Fig. 1B and Supplementary Figs. 1B and 2A). Taken together, EVs are enriched in CD73 and EpCAM. Therefore, we reasoned that EpCAM is a suitable target for tumor/EV-selective blockade of the CD73 immune checkpoint.

3.2. BsAb CD73xEpCAM has dual binding specificity for CD73 and EpCAM

BsAb CD73xEpCAM was constructed in a so-called bispecific taFv-Fc format [27] (Fig. 2A and B). SDS-PAGE analysis indicated that under both non-reducing (lane 1) and reducing (lane 2) conditions bsAb CD73xEpCAM migrated as a single protein band. This is in agreement with the disulfide-stabilized dimeric single-chained composition of bsAb CD73xEpCAM. CD73-blocking monospecific antibody oleclumab showed heterodimeric composition of heavy and light chain characteristics for conventional antibodies (lane 3 and 4) (Fig. 2C). BsAb CD73xEpCAM and oleclumab show comparable stability upon storage for up to 7 days in serum, at different pH conditions (pH 4–7), and at various temperatures (−20, 4, 37 °C) (Supplementary Fig. 3). Dual binding activity of bsAb CD73xEpCAM was confirmed by flow cytometry using Chinese Hamster Ovary (CHO) cells transfected with either CD73 or EpCAM (Supplementary Fig. 2B). Results demonstrate that only bsAb CD73xEpCAM bound dose-dependently to CHO.CD73 and CHO.EpCAM cells, and not to parental CHO cells (Fig. 2D, Supplementary Figs. 2C and 2D). Importantly, binding of bsAb CD73xEpCAM towards H292 cells was only partially reduced in the presence of excess amounts of soluble CD73 (sCD73), whereas excess amounts of soluble EpCAM (sEpCAM) strongly inhibited the binding. Of note, binding of bsAb CD73xEpCAM was only fully abrogated in the combined competing presence of sCD73 and sEpCAM (Fig. 2E), indicating bsAb CD73xEpCAM selectively and simultaneously binds to CD73 and EpCAM. Taken together, bsAb CD73xEpCAM has dual binding specificity for CD73 and EpCAM.

3.3. BsAb CD73xEpCAM potently inhibits the enzyme activity of CD73 on cancer cells and EVs in an EpCAM-directed manner

The dynamics of AMP hydrolysis by cancer cell- and EV-exposed CD73 were analyzed using H292 cells and corresponding EVs, respectively. To this end, increasing amounts of H292, H292$^{CD73-KO}$ cancer cells and corresponding EVs were incubated in medium supplemented with AMP. Inorganic phosphate (Pi) produced by CD73-mediated hydrolysis of the added AMP was evaluated using a colorimetric malachite green-based Pi assay. We observed that H292 cells and derived EVs displayed prominent CD73 enzyme activity, whereas H292$^{CD73-KO}$ cells and corresponding EVs were devoid of this activity (Fig. 3A and B). Next, we compared bsAb CD73xEpCAM and oleclumab for capacity to inhibit the enzyme activity of CD73 exposed on H292 cells and corresponding EVs. The results indicated that bsAb CD73xEpCAM outperformed oleclumab both for inhibiting CD73 on cells (~72% vs. ~53%, respectively) and EVs (~75% vs. ~35%, respectively) (Fig. 3C and D). Additionally, the CD73-inhibitory activity of bsAb CD73xEpCAM towards H292-derived EVs was strongly reduced in the presence of excess amounts of sEpCAM (Fig. 3E) and was limited towards EpCAM-KO EVs (Fig. 3F). Taken together, bsAb CD73xEpCAM has the unique capacity to potently inhibit the enzyme activity of CD73 exposed on both cancer cells and EVs and does so in an EpCAM-directed manner.

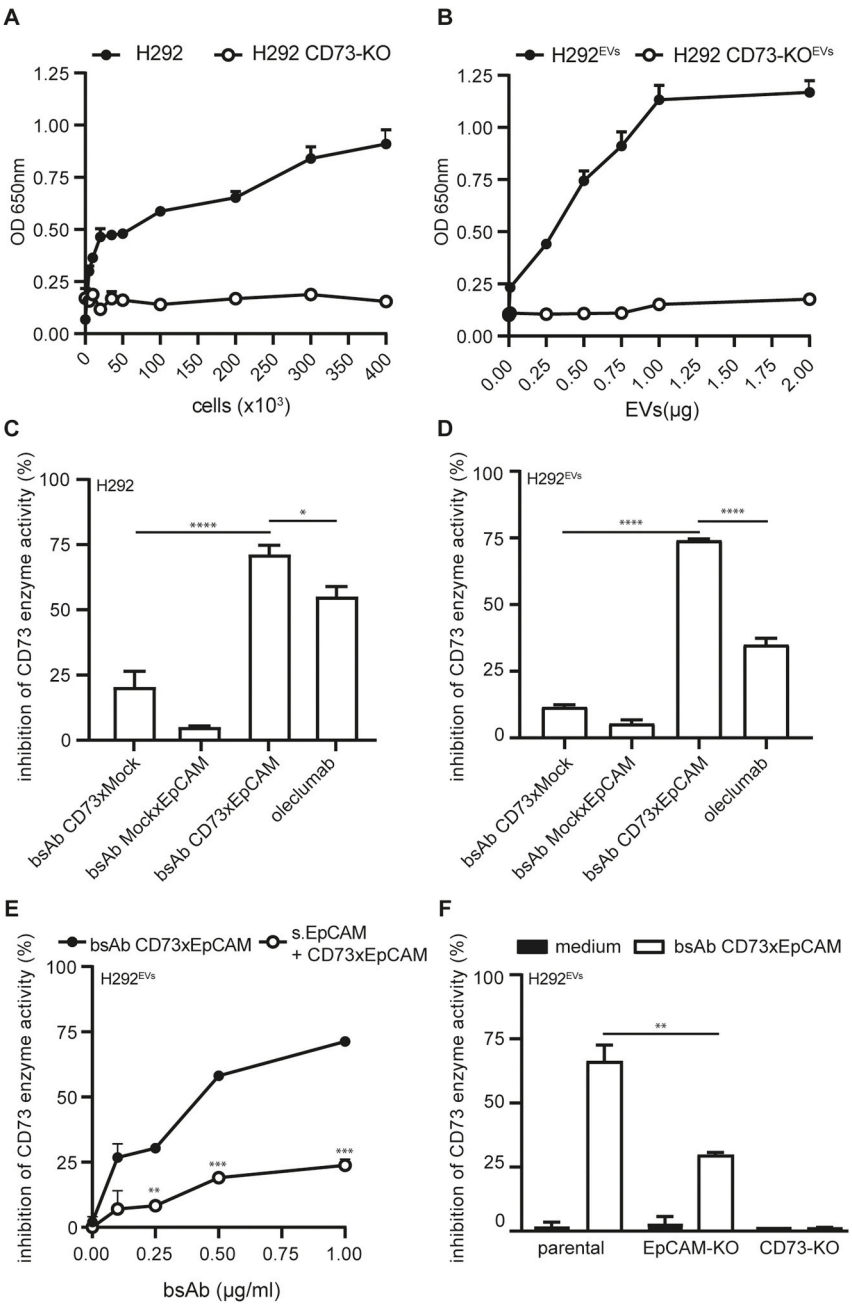

Fig. 3. BsAb CD73xEpCAM inhibits the enzyme activity of CD73 on cancer cells and EVs in an EpCAM-directed manner. (A–B) Increasing amounts of H292 and $H292^{CD73-KO}$ cancer cells or EVs were incubated with AMP (100 µM) and inorganic phosphate (Pi) produced by CD73-mediated hydrolysis of AMP was evaluated. (C–D) BsAb CD73xEpCAM, bsAb-controls or oleclumab (1 µg/ml) were added to H292 cancer cells or EVs and evaluated for capacity to inhibit the enzyme activity of CD73. Background levels of Pi in the absence of bsAb CD73xEpCAM was used to normalize CD73 inhibition to 0%. (E) Competitive CD73 enzyme inhibition assay in which bsAb CD73xEpCAM was pretreated with excess amounts of sEpCAM (10 µg) prior to incubation with H292-derived EVs and assessed for its capacity to inhibit the enzyme activity of CD73. (F) EpCAM-directed blockade of CD73 on H292-derived parental, EpCAM-KO and CD73-KO EVs using bsAb CD73xEpCAM (1 µg/ml). CD73-mediated hydrolysis of AMP into ADO was evaluated using a colorimetric malachite green-based Pi assay. All graphs represent mean ± SD. Statistical analysis in graphs C-D was performed using un-paired T test. Statistical analysis in graph E was performed using one-way ANOVA followed by a Tukey post-hoc test. Statistical analysis in graph F was performed using multiple T tests (*p < .05, **p < .01, ***p < .001, ****p < .0001).

3.4. BsAb CD73xEpCAM overcomes EV-induced suppression of T cell proliferation

We investigated the ability of $CD73^{pos}$ EVs to suppress T cell proliferation and the capacity of bsAb CD73xEpCAM and oleclumab to overcome this suppression. In short, CFSE-labeled PBMCs were incubated with H292 parental or CD73-KO EVs in medium supplemented with AMP. Next, T cells were stimulated to expand using activation beads and live cell imaging was used to quantify the size of activated T cell clusters over time (Fig. 4A). Activation beads promoted proliferation of T cells, whereas incubation with H292-derived EVs potently inhibited this proliferation. Importantly, CD73-KO EVs showed negligible capacity to inhibit the proliferative capacity of T cells. Next, we investigated whether bsAb CD73xEpCAM or oleclumab could overcome EV-suppressed T cell proliferation. Representative light-microscopy pictures shown in Fig. 4B indicated that bsAb CD73xEpCAM, but not oleclumab, fully abrogated the EV-mediated suppression of T cell proliferation as can be appreciated from a dramatic increase in size and number of T cell clusters. These results corroborated the quantification of the activated T cell clusters size in time (Fig. 4C). Incubation of PBMCs with H292-derived EVs and AMP resulted in a ~2-fold decrease in proliferation compared to activation beads only, and bsAb CD73xEpCAM fully restored the proliferative capacity of T cells (Fig. 4D). Taken together, bsAb CD73xEpCAM has potent capacity to overcome EV-induced suppression of T cell proliferation.

3.5. BsAb CD73xEpCAM restores the anticancer activity of EV-suppressed T cells

We investigated the ability of $CD73^{pos}$ EVs to suppress the anticancer activity of T cells and the capacity of bsAb CD73xEpCAM vs. oleclumab to restore this activity. To this end, PBMCs were cultured in medium supplemented with AMP in the presence (or absence) of H292 parental or CD73-KO EVs. Subsequently, cytotoxic T cells were stimulated and re-

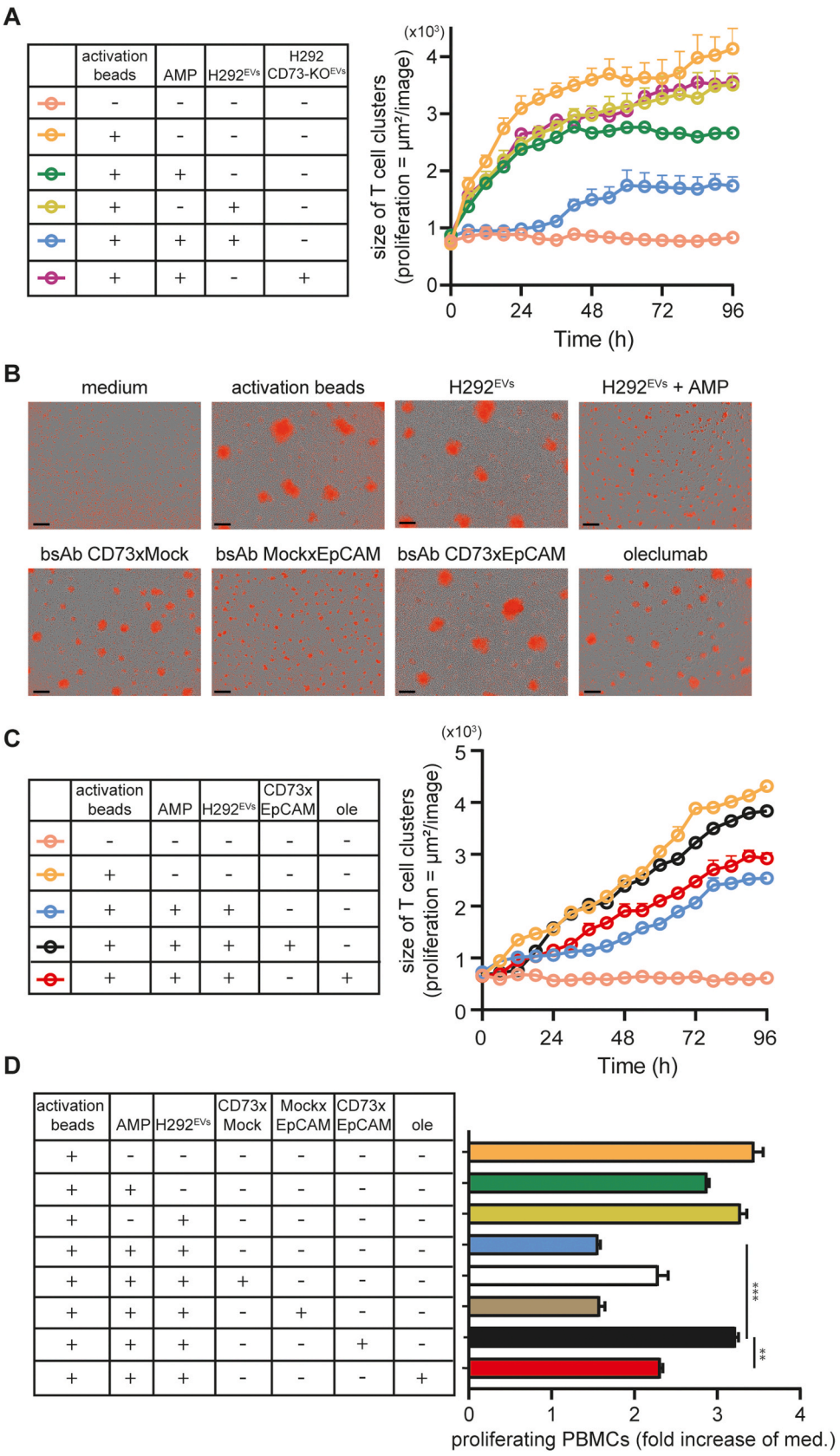

Fig. 4. BsAb CD73xEpCAM overcomes EV-mediated suppression of T cell proliferation. (A) PBMCs were labeled with CFSE and incubated with H292 parental and CD73KO-derived EVs (50 µg/10^6 PBMCs) at 37 °C for 3 d. Next, PBMCs were incubated with T cell activation beads in a bead-to-cell ratio of 2:1 in medium supplemented with AMP (100 µM). Live cell imaging technology was used to quantify the size of activated proliferating T cell clusters (µm²/image) by taking pictures every 1.5 h at 10x magnification at 37 °C for 4 d. (B–C) PBMCs were incubated with H292-derived EVs (50 µg/10^6 PBMCs) in the present or absence of bsAb CD73xEpCAM, bsAb-controls or oleclumab (1 µg/ml) at 37 °C for 3 d. Subsequently, PBMCs were activated in order to expand and analyzed as indicated above. Representative images were taken in B (time = 96 h, error bar = 400 µm) and quantified (µm²/image) over time in C. (D) The number of viable PBMCs was evaluated by Trypan blue staining using an automated cell counter. All graphs represent mean ± SD. Statistical analysis in graph D was performed using un-paired T test (**p < .01, ***p < .001). Ole = oleclumab in graphs C-D.

directed to kill EpCAM-expressing PC3M cancer cells using an EpCAM-directed/CD3-agonistic bispecific antibody (BIS-1) [26], in the presence of a conditionally fluorescent caspase 3/8 probe. Live cell imaging technology was used to assess the induction of apoptotic cancer cell death over time. Induction of cancer cell death, evident from high caspase-3/8 activation levels in target cells, dropped dramatically when cytotoxic T cells were incapacitated by subjecting them to AMP plus H292-derived EVs. Incubation with CD73-KO EVs only marginally reduced the anticancer activity of cytotoxic T cells (Fig. 5A). Importantly, bsAb CD73xEpCAM, but not oleclumab, restored the capacity of EV-suppressed T cells to kill cancer cells (Fig. 5B). These results corroborated ELISA data quantifying the restored capacity of these cytotoxic T cells to secrete IFN-γ (Fig. 5C). Taken together, bsAb CD73xEpCAM restores the capacity of EV-suppressed cytotoxic T cells to kill cancer cells.

3.6. BsAb CD73xEpCAM inhibits the enzyme activity of CD73 on cancer patient-derived EVs

Nanoscale vesicles were purified from rinsing fluid obtained during Hyperthermia Intraperitoneal Chemotherapy (HIPEC) surgery. Vesicle size distribution ranged from 117 nm to 176 nm (Fig. 6A and Supplementary Fig. 4). Immunoblot analysis revealed that TSG101 was present in vesicles from 6 out of 6 cancer patients (Fig. 6B). Additionally, 5 out of 6 cancer patient-derived EVs exposed CD73, which is in agreement with the respective OD_{650nm} values representing the enzyme activity of CD73 (Fig. 6B and C). Of note, only EVs derived from patient # 6 exposed both CD73 and EpCAM. As expected, bsAb CD73xEpCAM outperformed oleclumab for inhibiting the enzyme activity of EV-exposed CD73 from patient # 6 (~75% vs. ~55%, respectively) (Fig. 6D). Taken together, bsAb CD73xEpCAM potently inhibits the enzyme activity of $CD73^{pos}$/$EpCAM^{pos}$ cancer patient-derived EV-exposed CD73.

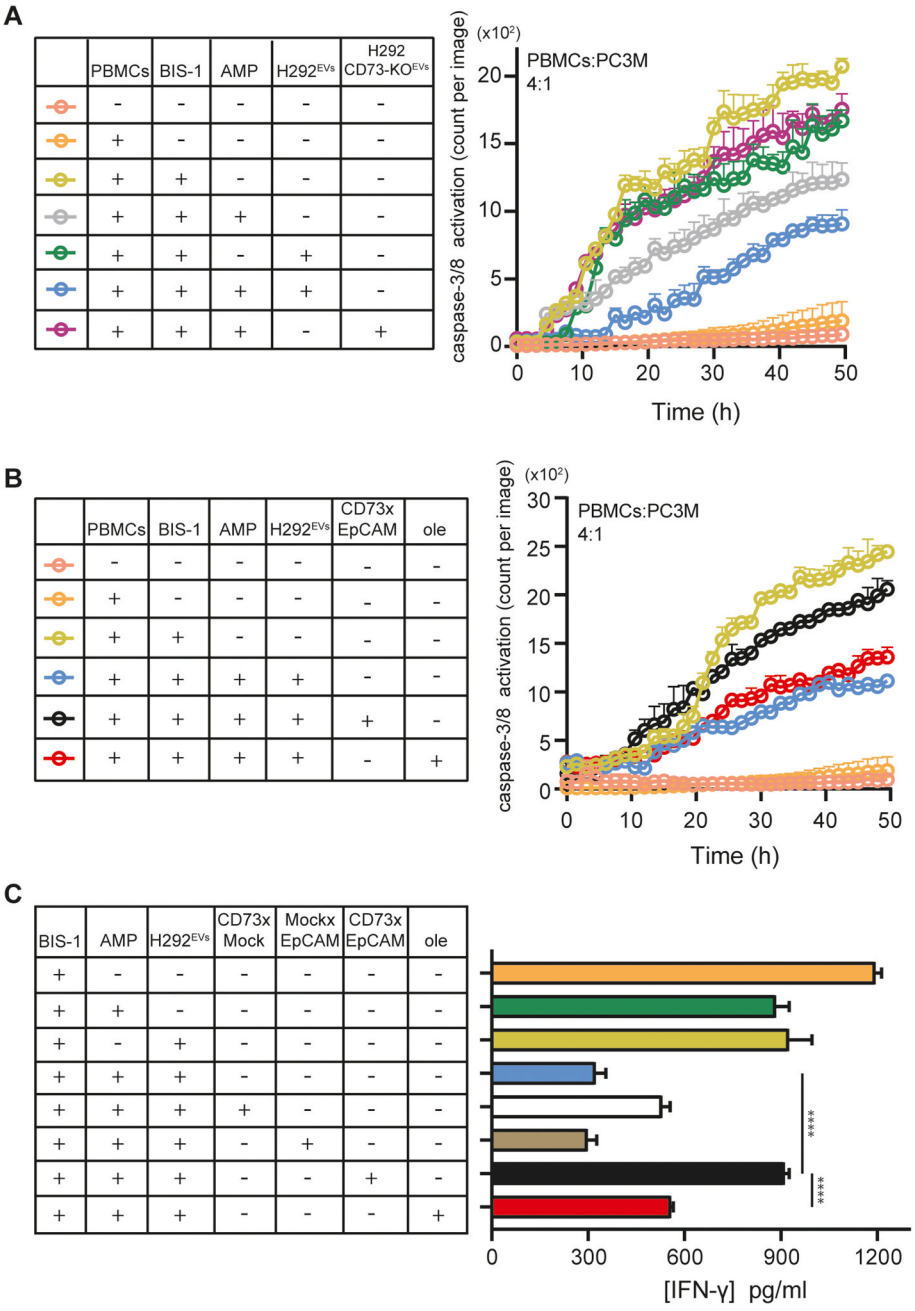

Fig. 5. BsAb CD73xEpCAM restores the anticancer activity of EV-suppressed PBMCs. (A) PBMCs were cultured in the presence, or absence, of $H292^{EVs}$ or H292 $CD73\text{-}KO^{EVs}$ (50 μg/10^6 PBMCs) at 37 °C for 3 d. Next, PBMCs were incubated (or not) with AMP (100 μM) at 37 °C for 24 h. Subsequently, cytotoxic T (Effector) cells were stimulated and re-directed to kill EpCAM-expressing PC3M (Target) cancer cells using BIS-1 in an effector (E) to target (T) cell ratio of 4:1. Subsequently, effector and target cells were co-cultured for 2 d in the presence of a conditionally fluorescent caspase 3/8–488 probe. Live cell imaging technology was used to evaluate induction of apoptotic cancer cell death (caspase-3/8 activation, count per image) by taking pictures every 1.5 h at 10x magnification at 37 °C for 2 d. (B) PBMCs were incubated with $H292^{EVs}$ (50 μg/10^6 PBMCs) in the present or absence of bsAb CD73xEpCAM, bsAb controls or oleclumab (1 μg/ml) at 37 °C for 3 d. Subsequently, PBMCs were incubated (or not) with AMP (100 μM) at 37 °C for 24 h and re-directed using BIS-1 to kill PC3M cancer cells. Using live cell imaging technology, apoptotic cell death was analyzed over time. (C) IFN-γ levels in culture supernatant of graph B were measured by ELISA. All graphs represent mean ± SD. Statistical analysis in graph C was performed using un-paired T test (****p < .0001). Ole = oleclumab in B and C.

A

colon carcinoma patient number	model size particles (nm)	concentration (10^6 particles/ml)
1	127.4 ± 7.3	182.20
2	158.8 ± 3.4	153.41
3	176.3 ± 6.6	186.11
4	168.7 ± 2.7	185.76
5	117.5 ± 4.3	48.05
6	157.5 ± 4.5	184.96

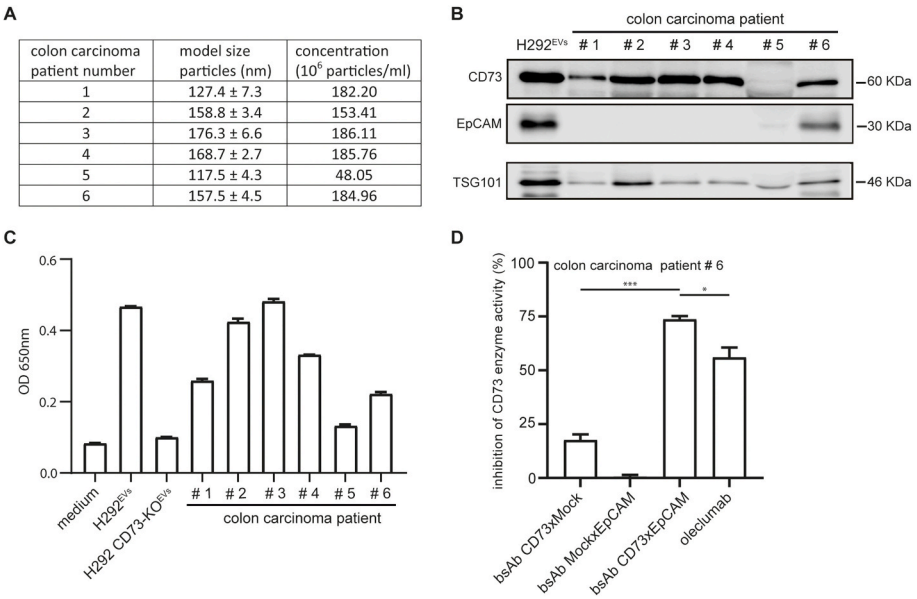

Fig. 6. BsAb CD73xEpCAM inhibits the enzyme activity of CD73 on cancer patient-derived EVs. (A) Characterization of colon carcinoma patient-derived EVs. (B) Representative immunoblotting images of the detection of CD73, EpCAM and TSG101 in cancer patient-derived EVs (20 μg). (C) Cancer patient-derived EVs were incubated with AMP (100 μM) and Pi produced by CD73-mediated hydrolysis of AMP was evaluated. (D) BsAb CD73xEpCAM, bsAb-controls or oleclumab (1 μg/ml) were added to EVs derived from patient # 6 and evaluated for capacity to inhibit the enzyme activity of CD73. Background levels of Pi present in the medium in the absence of bsAb CD73xEpCAM was used to normalize CD73 inhibition to 0%. All graphs represent mean ± SD. Statistical analysis in graph D was performed using un-paired T test (*p < .05, ***p < .001).

4. Discussion

Cancer cells exploit cell surface overexpression of the inhibitory immune checkpoint molecule CD73 to evade elimination by the immune system. Moreover, many cancer types excrete large amounts of CD73-exposing EVs, which further contributes to immune escape and tumor progression [5–7]. Therefore, strategies that inhibit both cancer cell-exposed and EVs-exposed CD73 may be of significant importance for cancer immunotherapy. Our data demonstrate that oleclumab, a clinically-relevant CD73-blocking antibody, has only limited capacity to block the enzyme activity of EVs-exposed CD73 and essentially fails to reactivate the proliferative and tumor cell-killing capacity of EVs-suppressed (anticancer) T cells. Apparently, conventional monospecific CD73-blocking antibodies lack sufficient binding avidity and tumor-selectivity.

Recently, we demonstrated that tumor-directed blockade of immune checkpoints PD-L1 and CD47 can be achieved using bsAb-based approaches [15–18]. In this study, we found that bsAbs appear to be better equipped to selectively block CD73 on cancer cells and corresponding EVs. BsAbs are an emerging class of recombinant therapeutic protein drugs that can be engineered to selectively target, modulate and interconnect biologic activities of otherwise separately acting surface receptors and ligands in a pre-designed manner [28]. Moreover, tetravalent bsAbs are known to have significantly enhanced avidity towards cells that simultaneously express both target antigens of interest, as they have up to four binding sites available for enhancement of functional interactions [29]. Thus, use of the tetravalent molecular format of bsAb CD73xEpCAM may result in an enhanced avidity towards carcinoma cells and carcinoma-derived EVs due to its capacity for multivalent interactions with the co-exposed CD73 and EpCAM molecules. Although not formally studied here, it is likely that the avidity characteristic of tetravalent bsAb CD73xEpCAM is the main mechanism-of-action for its unique capacity to efficiently and selectively antagonize the immunoinhibitory activity of CD73 exposed on carcinoma-derived EVs.

In the current study, we demonstrate that bsAb CD73xEpCAM blocks CD73 in an EpCAM-directed manner, both on carcinoma cells and EVs. The tumor-selective and inhibitory activity of bsAb CD73xEpCAM towards cancer cells and derived EVs strongly outperformed that of oleclumab. This remarkable activity of bsAb CD73xEpCAM is most likely attributable to its unique tetravalent, bispecific binding capacity for surface co-exposed CD73 and EpCAM.

Intriguingly, while selected carcinoma types showed relatively low levels of cell surface-exposed CD73, we detected that the corresponding EVs were strongly enriched in CD73 exposure. Moreover, based on protein content, we calculated that the AMP-to-ADO converting capacity of 0.75 μg EV may equal that of up to 400,000 of the originating cancer cells. Possibly, the locally increased density of CD73 exposure on EVs dramatically enhances its capacity to catalytically convert AMP to ADO. Alternatively, a variety of local factors, including (charged) lipid composition, pH and substrate concentration may also affect the enzyme activity of EV-exposed CD73. Nevertheless, bsAb CD73xEpCAM showed potent dose-dependent capacity to inhibit both cancer cell-exposed and EVs-exposed CD73 up to a maximum of ~75% (Fig. 3), whereas oleclumab CD73-inhibitory activity dropped to 35% on EVs. Moreover, bsAb CD73xEpCAM showed potent capacity to restore the anticancer activity of EV-suppressed T cells, whereas oleclumab essentially failed to do so.

Obviously, other immunosuppressive factors exposed on (e.g. PD-L1) and/or carried as cargo by EVs may not be inhibitable by bsAb CD73xEpCAM [30,31]. Indeed, it was previously demonstrated that EVs may expose TGF-β with an immunoinhibitory potency that exceeds that of its soluble form [32]. Luo et al. showed that breast cancer-derived EVs suppressed the proliferative capacity of T cells through EV-exposed TGF-β, which could be partly restored by neutralizing anti-TGF-β antibodies [33]. Additionally, it is noteworthy that it was recently uncovered that EVs not only expose CD73 to autonomously produce ADO, but may also directly deliver encapsulated ADO as part of their cargo. This EV-stored ADO represents a mechanism for delivery of cancer cell-produced ADO to distal sites that is fully independent of EV-exposed CD73 and thus cannot be inhibited by bsAb CD73xEpCAM [34]. The above advocates that the clinical efficacy of bsAb CD73xEpCAM may be enhanced when used in a combinatorial setting.

In the current study, we detected that EVs isolated from rinsing fluid obtained during HIPEC surgery of colon carcinoma patients showed significant CD73 enzyme activity. It is tentative to speculate that ADO-mediated immunosuppression may play a role in the highly malignant features of peritoneal carcinomatosis. In this respect, it is encouraging that bsAb CD73xEpCAM outperformed oleclumab by potently inhibiting CD73 exposed on EVs derived from a $CD73^{pos}$/$EpCAM^{pos}$ cancer patient.

In conclusion, bsAb CD73xEpCAM has unique abilities to [1]: simultaneously bind to both CD73 and EpCAM, resulting in enhanced avidity towards $CD73^{pos}$/$EpCAM^{pos}$ cancer cells and corresponding EVs [2]; inhibit the enzyme activity of CD73 on cancer cells and ($EpCAM^{pos}$

patient-derived) EVs in an EpCAM-directed manner [3]; overcome EVs-mediated suppression of T cell proliferation; and [4] restore the anticancer activity of EVs-suppressed cytotoxic T cells.

Taken together, the use of bsAb CD73xEpCAM may represent a promising strategy for cancer-directed blockade of the CD73-ADO immune checkpoint and may be of value to cancer immunotherapy of various EV-producing carcinomas.

Author contributions

Emily M. Ploeg: Formal analysis, Investigation, Resources, Validation, Writing – original draft. Xiurong Ke: Formal analysis, Investigation, Validation, Writing – original draft. Isabel Britsch: Data curation, Statistical analysis, Discussion. Mark A. J. M. Hendriks: Data curation, Statistical analysis, Discussion. Femke A. Van der Zant: Project administration, Resources. Schelto Kruijff: Project administration, Resources. Douwe F. Samplonius: Conceptualization, Project administration, Methodology, Investigation. Hao Zhang: Formal analysis, Discussion, Writing – review & editing. Wijnand Helfrich: Conceptualization, Formal analysis, Investigation, Methodology, Project administration, Validation, Writing – original draft, Writing – review & editing. All the authors read and approved the final manuscript.

Funding

This work was supported by the Dutch Cancer Society project numbers 11464 & 6986 (to W.H.) and Abel Tasman Talent Program (ATTP) Sandwich PhD Scholarship supported by the Graduate School of Medical Sciences of the University of Groningen (to X. K).

Declaration of competing interest

The authors declare that they have no known competing financial interests or personal relationships that could have appeared to influence the work reported in this paper.

Appendix A. Supplementary data

Supplementary data to this article can be found online at https://doi.org/10.1016/j.canlet.2021.08.037.

References

[1] V.O. Shender, M.S. Pavlyukov, R.H. Ziganshin, G.P. Arapidi, S.I. Kovalchuk, N. A. Anikanov, et al., Proteome-metabolome profiling of ovarian cancer ascites reveals novel components involved in intercellular communication [Internet], Mol. Cell. Proteomics 13 (12) (2014 Dec 1) 3558–3571. Available from: http://www.ncbi.nlm.nih.gov/pubmed/25271300.

[2] A. Zebrowska, A. Skowronek, A. Wojakowska, P. Widlak, M. Pietrowska, Metabolome of exosomes: focus on vesicles released by cancer cells and present in human body fluids, Int. J. Mol. Sci. 20 (14) (2019 Jul 2).

[3] M.W. Graner, O. Alzate, A.M. Dechkovskaia, J.D. Keene, J.H. Sampson, D. A. Mitchell, et al., Proteomic and immunologic analyses of brain tumor exosomes, Faseb. J. 23 (5) (2009 May) 1541–1557.

[4] T.L. Whiteside, Exosomes carrying immunoinhibitory proteins and their role in cancer, Clin. Exp. Immunol. 189 (2017) 259–267. Blackwell Publishing Ltd.

[5] A. Clayton, S. Al-Taei, J. Webber, M.D. Mason, Z. Tabi, Cancer exosomes express CD39 and CD73, which suppress T cells through adenosine production, J. Immunol. 187 (2) (2011 Jul 15) 676–683.

[6] P.J. Schuler, Z. Saze, C.S. Hong, L. Muller, D.G. Gillespie, D. Cheng, et al., Human CD4+CD39+ regulatory T cells produce adenosine upon co-expression of surface CD73 or contact with CD73+ exosomes or CD73+ cells, Clin. Exp. Immunol. 177 (2) (2014) 531–543.

[7] N. Ludwig, S.S. Yerneni, J.H. Azambuja, D.G. Gillespie, E.V. Menshikova, E. K. Jackson, et al., Tumor-derived exosomes promote angiogenesis via adenosine A2B receptor signaling, Angiogenesis 23 (4) (2020 Nov 1) 599–610.

[8] D. Allard, B. Allard, P.O. Gaudreau, P. Chrobak, J. Stagg, CD73-adenosine: a next-generation target in immuno-oncology, Immunotherapy 8 (2016) 145–163. Future Medicine Ltd.

[9] L. Antonioli, C. Blandizzi, F. Malavasi, D. Ferrari, G. Haskó, Anti-CD73 immunotherapy: a viable way to reprogram the tumor microenvironment, OncoImmunology 5 (2016). Taylor and Francis Inc.

[10] P. de A. Mello, R. Coutinho-Silva, L.E.B. Savio, Multifaceted effects of extracellular adenosine triphosphate and adenosine in the tumor-host interaction and therapeutic perspectives, Front. Immunol. 8 (2017). Frontiers Media S.A.

[11] C.M. Hay, E. Sult, Q. Huang, K. Mulgrew, S.R. Fuhrmann, K.A. McGlinchey, et al., Targeting CD73 in the tumor microenvironment with MEDI9447, OncoImmunology 5 (8) (2016 Aug 2).

[12] J.L. Hood, S. San Roman, S.A. Wickline, Exosomes released by melanoma cells prepare sentinel lymph nodes for tumor metastasis, Canc. Res. 71 (11) (2011 Jun 1) 3792–3801.

[13] J. Yang, F. Wei, C. Schafer, D.T.W. Wong, Detection of tumor cell-specific mRNA and protein in exosome-like microvesicles from blood and saliva, PloS One 9 (11) (2014 Nov 14).

[14] E. Schneider, A. Rissiek, R. Winzer, B. Puig, B. Rissiek, F. Haag, et al., Generation and function of non-cell-bound CD73 in inflammation, Front. Immunol. 10 (2019) 1729. NLM (Medline).

[15] I. Koopmans, M.A.J.M. Hendriks, R.J. van Ginkel, D.F. Samplonius, E. Bremer, W. Helfrich, Bispecific antibody approach for improved melanoma-selective PD-L1 immune checkpoint blockade, J. Invest. Dermatol. 139 (11) (2019 Nov 1) 2343–2351, e3.

[16] P.E. van Bommel, Y. He, I. Schepel, M.A.J.M. Hendriks, V.R. Wiersma, R.J. van Ginkel, et al., CD20-selective inhibition of CD47-SIRPα "don't eat me" signaling with a bispecific antibody-derivative enhances the anticancer activity of daratumumab, alemtuzumab and obinutuzumab, OncoImmunology 7 (2) (2018 Feb 1).

[17] I. Koopmans, D. Hendriks, D.F. Samplonius, R.J. van Ginkel, S. Heskamp, P. J. Wierstra, et al., A novel bispecific antibody for EGFR-directed blockade of the PD-1/PD-L1 immune checkpoint, OncoImmunology 7 (8) (2018 Aug 3).

[18] M.A.J.M. Hendriks, E.M. Ploeg, I. Koopmans, I. Britsch, X. Ke, D.F. Samplonius, et al., Bispecific antibody approach for EGFR-directed blockade of the CD47-SIRPα "don't eat me" immune checkpoint promotes neutrophil-mediated trogoptosis and enhances antigen cross-presentation, OncoImmunology 9 (1) (2020 Jan 1).

[19] P.T. Went, A. Lugli, S. Meier, M. Bundi, M. Mirlacher, G. Sauter, et al., Frequent EpCam protein expression in human carcinomas, Hum. Pathol. 35 (1) (2004) 122–128.

[20] S. Runz, S. Keller, C. Rupp, A. Stoeck, Y. Issa, D. Koensgen, et al., Malignant ascites-derived exosomes of ovarian carcinoma patients contain CD24 and EpCAM, Gynecol. Oncol. 107 (3) (2007 Dec) 563–571.

[21] P. Amrollahi, M. Rodrigues, C.J. Lyon, A. Goel, H. Han, T.Y. Hu, Ultra-sensitive automated profiling of EpCAM expression on tumor-derived extracellular vesicles, Front. Genet. (2019 Dec 17) 10.

[22] J.P. Zhang, X.L. Li, A. Neises, W. Chen, L.P. Hu, G.Z. Ji, et al., Different effects of sgRNA length on CRISPR-mediated gene knockout efficiency, Sci. Rep. (2016 Jun 24) 6.

[23] J. Yang, T. Isaji, G. Zhang, F. Qi, C. Duan, T. Fukuda, et al., EpCAM associates with integrin and regulates cell adhesion in cancer cells, Biochem. Biophys. Res. Commun. 522 (4) (2020 Feb 19) 903–909.

[24] W. Helfrich, H.J. Haisma, V. Magdolen, T. Luther, V.J.J. Bom, J. Westra, et al., A rapid and versatile method for harnessing scFv antibody fragments with various biological effector functions, J. Immunol. Methods 237 (1–2) (2000 Apr 3) 131–145.

[25] O. Vafa, G.L. Gilliland, R.J. Brezski, B. Strake, T. Wilkinson, E.R. Lacy, et al., An engineered Fc variant of an IgG eliminates all immune effector functions via structural perturbations, Methods 65 (1) (2014 Jan 1) 114–126.

[26] B.J. Kroesen, G.J. Wellenberg, A. Bakker, W. Helfrich, T.H. The, L. De Leij, The role of apoptosis in bispecific antibody-mediated T-cell cytotoxicity, Br. J. Canc. 73 (6) (1996) 721–727.

[27] U. Brinkmann, R.E. Kontermann, The making of bispecific antibodies, mAbs 9 (2017) 182–212. Taylor and Francis Inc.

[28] Y. Mazor, A. Hansen, C. Yang, P.S. Chowdhury, J. Wang, G. Stephens, et al., Insights into the molecular basis of a bispecific antibody's target selectivity, mAbs 7 (3) (2015 Jan 1) 461–469.

[29] Dong J, Sereno A, Aivazian D, Langley E, Miller BR, Snyder WB, et al. A stable IgG-like bispecific antibody targeting the epidermal growth factor receptor and the type I insulin-like growth factor receptor demonstrates superior anti-tumor activity. MAbs [Internet]. 3(3):273-288. Available from: http://www.ncbi.nlm.nih.gov/pubmed/21393993.

[30] M. Poggio, T. Hu, C.C. Pai, B. Chu, C.D. Belair, A. Chang, et al., Suppression of exosomal PD-L1 induces systemic anti-tumor immunity and memory, Cell 177 (2) (2019 Apr 4) 414–427, e13.

[31] G. Chen, A.C. Huang, W. Zhang, G. Zhang, M. Wu, W. Xu, et al., Exosomal PD-L1 contributes to immunosuppression and is associated with anti-PD-1 response, Nature 560 (7718) (2018 Aug 16) 382–386.

[32] J.P. Webber, L.K. Spary, A.J. Sanders, R. Chowdhury, W.G. Jiang, R. Steadman, et al., Differentiation of tumour-promoting stromal myofibroblasts by cancer exosomes, Oncogene 34 (3) (2015 Jan 15) 319–333.

[33] L. Rong, R. Li, S. Li, R. Luo, Immunosuppression of breast cancer cells mediated by transforming growth factor-β in exosomes from cancer cells, Oncol. Lett. 11 (1) (2016 Jan 1) 500–504.

[34] N. Ludwig, E.K. Jackson, T.L. Whiteside, Role of exosome-associated adenosine in promoting angiogenesis, Vessel Plus (2020 Apr 10) 2020.